Mediterranean Archaeology and Archaeometry, Vol. 13, No 3, pp. 155-161

PRELIMINARY RESULTS ON STRUCTURAL STATE CHARACTERIZATION OF K-FELDSPARS BY USING THERMOLUMINESCENCE

G.S. Polymeris[1,2], E. Theodosoglou[4], G. Kitis[3], N.C. Tsirliganis[1], A. Koroneos[4], K.M. Paraskevopoulos[2]

[1]Laboratory of Radiation Applications and Archaeological Dating, Department of Archaeometry and Physicochemical Measurements, 'Athena' - Research and Innovation Center in Information, Communication and Knowledge Technologies, Kimmeria University Campus, GR-67100, Xanthi, Greece

[2]Solid State Section, Department of Physics,

[3]Nuclear and Elementary Particle Physics Laboratory, Department of Physics,

[4]Department of Mineralogy – Petrology – Economic Geology, School of Geology, Aristotle University of Thessaloniki, 54124 Thessaloniki – Greece

Received: 21/11/2012
Accepted: 19/09/2013
Corresponding author: polymers@auth.gr

ABSTRACT

Feldspars are amongst the most widely used minerals for luminescence dating, besides having certain drawbacks such as anomalous fading. The present study attempts, for the first time in the literature, a direct correlation between the thermoluminescent intensity and specific structural parameters of alkali feldspars, such as the probability of Al-cation to occupy specific sites in the forming tetrahedra and the volume of the unit cell. The TL intensity was studied in the present study, in both terms of integrated signal throughout the entire glow curve region, as well as TL peak resolved integral following de-convolution analysis. In both terms, the TL intensity was found to be extremely sensitive to the aforementioned structural parameters. Moreover, the TL signal of the deconvolved shallow TL peak (termed as P1 throughout the text) was proved to be a diagnostic tool towards discriminating among the three phases of K-feldspars, namely sanidine, orthoclase and microcline, besides X-Rays and Transmission Electron Microscopy.

KEYWORDS: K-feldspars, sanidine, orthoclase, microcline, TL

1. INTRODUCTION

The group of feldspars stands amongst the most common and examined rock-forming mineral groups, as feldspars can be found in all rock types, igneous, sedimentary and metamorphic. They have aluminosilicates framework and their general formula is AT_4O_8, where T represents small-sized cations mostly (Si^{4+}, Al^{+3}). A stands mainly for charge compensating cations (Na^+, K^+, Ca^{2+}, Ba^{2+}) which occupy large, irregular cavities in the tetrahedral framework (Ribbe, 1983; Krbetschek et al., 1997). There are two main solid solution series in the group, alkali feldspars with end members $KAlSi_3O_8$ (K-feldspars) and $NaAlSi_3O_8$ and plagioclases with end members $CaAl_2Si_2O_8$ and $NaAlSi_3O_8$. Feldspars with K and Na in the A site form a continuous solid solution series at high temperatures, on slow cooling un-mixing takes place and the isomorphous series is destroyed. The solid solution is separated into two phases, one K-rich and the other one Na-rich. The new texture generated from this un-mixing is called cryptoperthitic, microperthitic or perthitic, depending on the size on the Na-rich areas (Deer et al., 1971; Smith and Brown, 1988).

The basic structure of an alkali feldspar consists of a three dimensional array of corner-sharing AlO_4 and SiO_4 tetrahedra. Three out of the four T cation sites in their unit cell are occupied by Si-cation and the fourth by Al-cation. The high temperature form of $KAlSi_3O_8$ is sanidine and is monoclinic (C2/m) with highly disordered distribution of Al/Si cations in the four T ($2T_1$, $2T_2$) sites, while the low temperature form, called microcline, is triclinic ($C\bar{1}$) with highly ordered distribution of Al/Si cations among the four sites (T_10, T_1m, T_20, T_2m). Most microcline samples show fine-scale tartan twinning, and the variety orthoclase, once regarded as a homogenous K-feldspar with intermediate order between sanidine and microcline, is now known to have a complex "tweed" texture revealed by high resolution electron microscopy, but which is so fine that optical and even X-ray methods yield in effect "average" properties. In this sense orthoclase is perceived as monoclinic (C2/m) in structure and as having monoclinic optical parameters between those of microcline and sanidine (Smith and Brown, 1988; Deer et al., 2001).

In the most ordered structural state of microcline, Al cation occupies the T_10 and Si the T_1m, T_20 and T_2m sites, while in the most disordered structural state of sanidine each one of the T sites has the same probability to be occupied by the Al cation. The probability of Al cation to occupy one of the T sites is expressed by t_10, t_1m, t_20 and t_2m and t_1 and t_2 for the T_10, T_1m, T_20 and T_2m and T1 and T2 sites of triclinic and monoclinic species, respectively. Sanidine, representing the completely disordered form, yields $2t_1=2t_2=0.5$, while microcline, the completely ordered one yields $t_10=1.0$ and $t_1m=t_20=t_2m=0.0$. Orthoclase stands as an intermediate form with $t_10+t_1m>t_20+t_2m$.

Feldspars stand among the most widely used minerals for luminescence dating, besides certain drawbacks such as anomalous fading (Wintle, 1973; Huntley and Lamothe, 2001). Several studies were carried out concerning their composition and structure, after applying a variety of methods, such as X-Ray Powder Diffraction (XRPD, Kroll and Ribbe, 1983; Theodosoglou et al., 2010), Fourier Transformed Infrared Spectroscopy (FTIR, Zhang et al., 1997), Transmission Electron Microscopy (TEM, Lee et al., 2007), etc. Nevertheless, the use of luminescence has been so far restricted to age assessment. The aim of the present paper is to examine whether thermoluminescence (TL) could be used as a diagnostic tool for structural state characterization in the case of K-feldspars. Previous works on the specific topic are scarce, considering the influence of the structural parameters on the luminescence properties of feldspars (Correcher et al., 2000; Garcia-Guinea et al., 2007). The main question which is to be answered is whether luminescence could be directly correlated to microscopically-estimated (e.g. by XRD) structural parameters of feldspars, such as the probability of Al-cation to occupy the T1 sites (Σt_1) and the volume of the unit cell.

2. MATERIALS AND METHODS

The samples used are ten naturally occurring K-feldspars from igneous rocks of Northern Greece. The K-feldspars were separated from the mafic and felsic minerals with the use of Franz (model L-1) magnetic separator and Sodium Po-

lytungstate (SPT) heavy liquid, respectively. The purity of K-feldspars was identified and classified based on XRPD measurements. The XRPD patterns were obtained on a PHILIPS PW 1820/00 X-ray diffractometer of the Department of Mineralogy-Petrology-Economic Geology, School of Geology, A.U.Th., carrying a PW 1710 microprocessor and using PC-APD software.

Operating conditions for all samples were 35 kV and 25 mA using Ni-filtered Cu $K_{\alpha ave}$ radiation. The 2theta (2θ) scanning range was between 3 and 63° and the scanning speed was 0.6° min^{-1}. The identification of the samples was made using the JCPDS-ICDD 2003 database. Their unit cell parameters, as well as the refinements were calculated with CHEKCELL (Laugier and Bochu, 2001) software. The probability of Al-cation occupying one of the T1 sites ($\Sigma t_1 = t_1 0 + t_1 m$) was calculated using the equations of Kroll and Ribbe (1987). According to the XRPD patterns of the examined samples, they are divided in three species: sanidine, orthoclase and microcline. It should be noted that the Σt_1 has the lowest values for sanidine and the highest for microcline, while orthoclase have intermediate values. Therefore, the examined samples were selected in order to cover the entire region of the potential Σt_1 values.

All luminescence measurements were performed using a RISØ TL/OSL reader (model TL/OSL DA-15), equipped with a 0.0785 Gy s^{-1} $^{90}Sr/^{90}Y$ β-ray source (Bøtter-Jensen et al., 2000). The reader is fitted with an EMI 9635QA PM Tube. Unless otherwise stated, all TL measurements were performed using a Hoya U-340 filter (270–380 nm). A heating rate of 1°C s^{-1} was used in all TL readouts in order to minimize significant temperature lag, up to a maximum temperature of 500°C. The test dose applied was 25 Gy in all cases.

A Computerized Curve Deconvolution Analysis (CCDA) was performed in the case of TL glow curves for a peak-resolved analysis. The single glow-peak equation of general order kinetics was used:

$$I(T) = I_m \cdot b^{\frac{b}{b-1}} \exp\left(\frac{E}{kT}\frac{T-T_m}{T_m}\right) \cdot \left[(b-1)(1-\Delta)\frac{T^2}{T_m^2}\exp\left(\frac{E}{kT}\frac{T-T_m}{T_m}\right) + Z_m\right]^{-\frac{b}{b-1}} \quad (1)$$

$$\text{Where } \Delta = 2kT/E,\ \Delta_m = 2kT_m/E \text{ and } Z_m = 1+(b-1)\cdot\Delta_m. \quad (2)$$

Equation (1), suggested by Kitis et al. (1998), is an analytical expression that could be used for CCDA in the case of single-value energy trap depth associated with the localized states, with each crystalline phase corresponding to a discrete trap distribution. All curve fittings were performed using the software package Microsoft Excel, with the Solver utility (Afouxenidis et al., 2012), while the goodness of fit was tested using the Figure of Merit (FOM) of Balian and Eddy (1977). The obtained FOM values were between 0.8% and 2.5%.

3. RESULTS AND DISCUSSION

Specific TL properties, such as glow curve shape and sensitivity, were studied in order to be correlated to their unit cell parameters, i.e. the probability of Al cation to occupy one of the T1 sites ($\Sigma t_1 = t_1 0 + t_1 m$) and the volume of the unit cell corresponding to their structural state. The same mass was used for all samples, in order to compare the sensitivity among the different minerals. Reproducibility in masses of all subsamples was strictly kept within 2%.

Table 1 presents, for each sample, the unit cell volume based on the unit cell parameters that were calculated, as well as the probability of Al-cation to occupy one of the T_1 sites ($\Sigma t_1 = t_1 0 + t_1 m$).

Table 1: The volume of unit cell along with the probability Σt_1 for each K-feldspar sample subjected to the present study.

A/A	Lab. Code Name	Unit Cell Volume (Å³)	Probability $t_1 0 + t_1 m$
1	SAM2	698.52	0.50
2	BAL21	707.47	0.58
3	SAM3	708.55	0.60
4	MRK4	711.92	0.69
5	VRS4	716.23	0.80
6	VRS8	715.05	0.89
7	VRS3	718.98	0.94
8	XAN8	719.22	0.93
9	ELD1	719.45	0.96
10	KST4	720.51	1.00

The XRPD spectra from which the data in Table 1 were calculated are presented in Fig. 1.

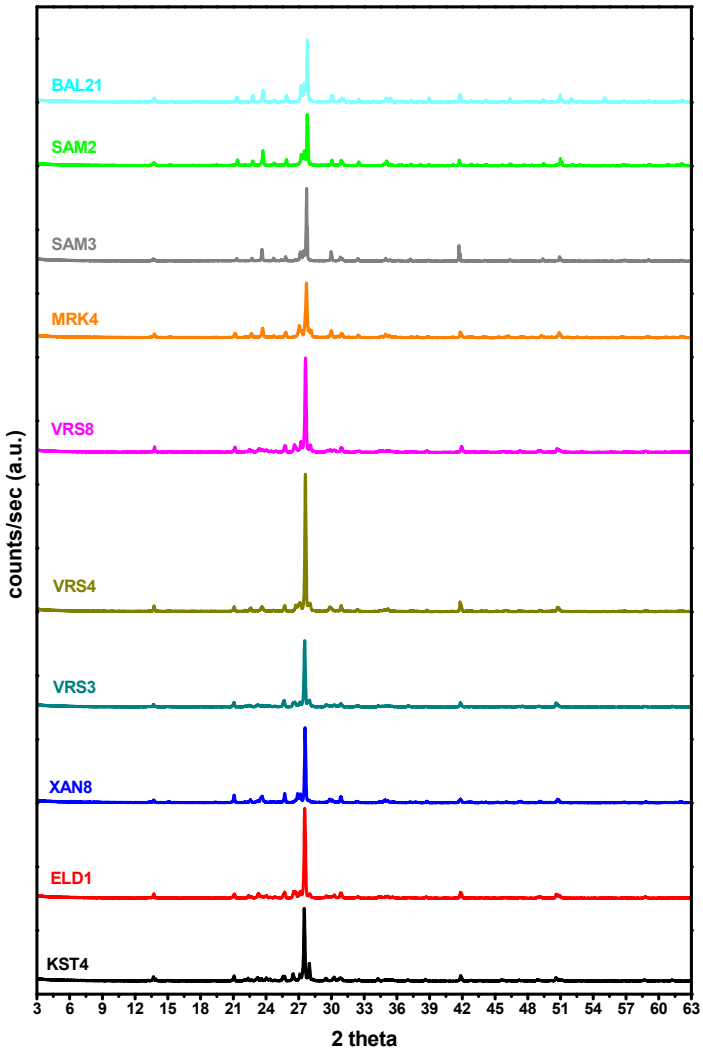

Figure 1. XRPD Patterns of the examined samples.

There is a monotonically increasing behaviour between the latter and the unit cell volume (apart from VRS8 for the case of unit cell volume and XAN8 for the case of probability).

However, different species of K-feldspars can be found, presenting the same unit cell volume values, in case of stressed crystals. TL glow curves for a selection of feldspars, measured promptly after artificial irradiation, are presented in Fig. 2.

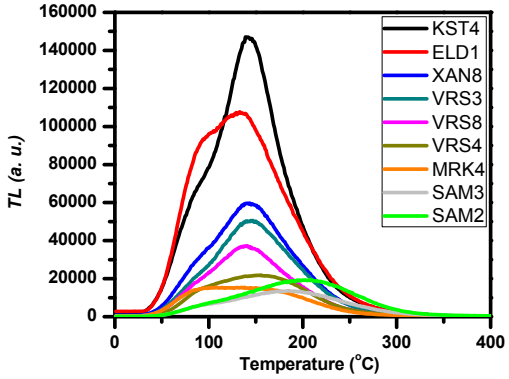

Figure 2: TL glow curves for 9 out of the 10 feldspar samples under study. The mass and the dose is the same for all samples in order to check for sensitivity variations.

It becomes obvious that the intensity, in terms of the integral throughout the entire glow curve, increases for increasing unit cell volume (thus for increasing probability Σt_1 as well). This is the first and most interesting straightforward correlation between the macroscopically measured TL intensity and the microscopically estimated volume of the unit cell.

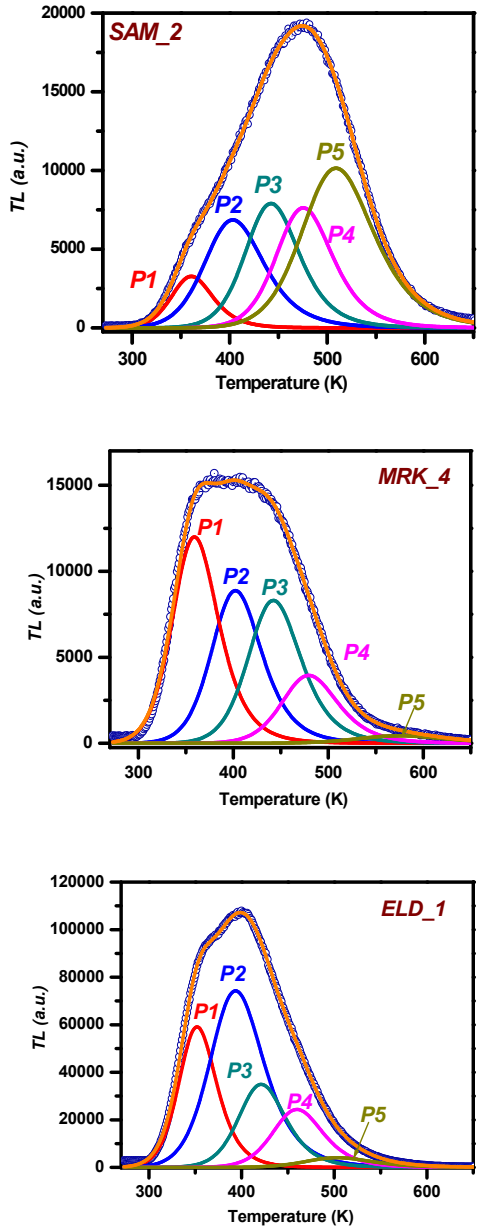

Figure 3. TL glow curves for three different feldspar samples, de-convolved into their 5 individual peaks, labeled as P1 – P5. Open dots correspond to experimentally obtained glow curves, while continuous lines correspond to fitting results.

Besides yielding different intensities, the TL glow curves of all samples exhibit similar shapes. This similarity was also established based on the de-convolution results. For all samples, 5 different individual glow peaks were applied, labelled as P1 – P5. TL glow curves for three different feldspar samples, de-convolved into their individual peaks are presented in Fig. 3.

According to equation 1, there are four fitting parameters, namely I_{max}, E, b and T_{max}. The three latter fitting parameters (E, b, T_{max}) of each glow peak were reproducible for all feldspar samples within 3.1%. One slight exception appears with respect to the de-convolution results concerning the glow peak P5. Even though this TL peak is present in the de-convolution results of all samples, its intensity is much more enhanced for the feldspars of the sanidine group (low values of Σt_1), while at the same time its T_{max} value some lower. This is a result that can be easily observed from both Figs 3 and 4. The latter presents the integrated TL intensity of the glow peaks P1, P4 and P5 versus the probability $\Sigma t_1 = t_10+t_1m$. The behavior of the intensity of both peaks P2 and P3 is similar to that of P4; therefore it is not presented in Fig. 4. For four among the five TL peaks, the integrated intensity after de-convolution is monotonically increasing with probability Σt_1. Only the TL glow peak P5 is decreasing while this latter probability increases. Similar results are yielded even if the integrated TL intensities will be plotted versus the unit cell volume.

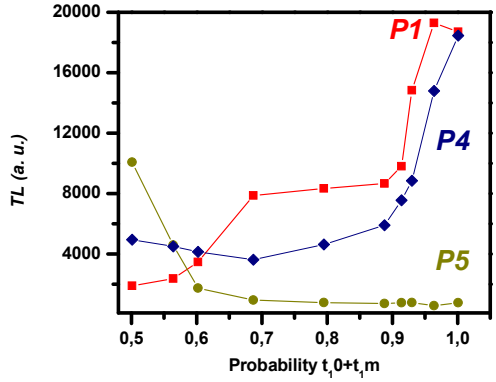

Figure 4. Integrated TL intensity of glow peaks P1, P4 and P5 versus the probability $\Sigma t_1 = t_10+t_1m$. The behavior of intensity of both P2 and P3 is similar to that of P4.

As Fig. 4 further reveals, the integrated intensity of the presented glow peaks were proved to be very sensitive to discriminating among the feldspars of different forms.

In fact, glow peak P5 is very sensitive to sanidine, due to the increased integral for the samples belonging to the corresponding group. Similarly, the integrated intensity of glow peaks P3 and P4 is much changing for the cases of feldspars belonging to the group of microcline. However, the most interesting result arises from the response of TL glow peak P1 versus Σt_1, clearly demonstrating three different, well distinguished parts.

Each part corresponds to a specific group-form of K-feldspars, namely an increasing region for low values of Σt_1 (namely sanidine), a plateau for the orthoclase with intermediate values of Σt_1 as well as a further increasing part corresponding to microcline with Σt_1 values tending to unity.

Put simply, the normalized integrated intensity of the TL peak P1 could be effectively used towards establishing one calibration curve of prevalent nature for all K-feldspars, towards discriminating between samples belonging to different groups.

4. CONCLUSIONS

The preliminary results so far suggest that there is a straightforward correlation between the macroscopically measured TL intensity and the microscopically estimated structural characteristics of K-feldspars, such as the volume of the unit cell as well as the probability of Al-cation to occupy one of the T1 sites (Σt_1). Deconvolution of the corresponding TL signal could also provide with a useful diagnostic tool towards discriminating between the three phases of K-feldspars, namely sanidine, orthoclase and microcline. Further work is required in order to study more luminescent properties, such as IRSL and anomalous fading, of more samples towards the formation of a calibration curve of prevalent nature.

REFERENCES

Afouxenidis, A., Polymeris, G.S., Tsirliganis, N.C., Kitis, G. (2012) Computerized curve deconvolution of TL/OSL curves using a popular spreadsheet program. *Radiation Protection Dosimetry*, vol. 149 (4), 363-370.

Balian, H.M., Eddy, N.W. (1977) Figure Of Merit (FOM). An improved criterion over the normalized Chi-squared test for assessing goodness of fit of gamma-ray spectral peaks. *Nuclear Instruments and Methods*, vol. 145, 389-395.

Bøtter-Jensen, L., Bulur, E., Duller, G.A.T., Murray, A.S. (2000) New advances in luminescence dating. *Radiation Measurements*, vol. 32, 523–528.

Correcher, V., Garcia-Guinea, J., Delgado, A. (2000) Influence of preheating treatment on the luminescence properties of adularia feldspar ($KAlSi_3O_8$). *Radiation Measurements*, vol. 32, 709 – 715.

Deer, W.A., Howie, R.A., Zussman, J. (1971) *Rock forming minerals*, vol. 4. Framework silicates. London, Longman Group, 435pp.

Garcia-Guinea, J., Correcher, V., Delgado, A., Sanchez-Mûnoz, L. (2000) Cluster linkages between luminescence emission spectra and continuous trap distribution in a volcanic sanidine. *Radiation Measurements*, vol. 37, 473 – 477.

Huntley, D.J., Lamothe, M. (2001) Ubiquity of anomalous fading in K-feldspars and the measurement and correction for it in optical dating. *Canadian Journal of Earth Science*, vol. 38, 1093–1106.

Kitis, G., Gomez-Ros, J.M., Tuyn, J.W. (1998) Thermoluminescence glow-curve deconvolution functions for first, second and general orders of kinetics. *Journal of Physics D: Applied Physics*, vol. 31, 2636-2641.

Krbetschek, M.R., Gotze, J., Dietrich, A., Trautmann, T. (1997) Spectral information from minerals relevant for luminescence dating. *Radiation Measurements*, vol. 27 (5-6), 695 – 748.

Kroll H., Ribbe P.H. (1983) Lattice parameters, composition and Al, Si order in alkali feldspars. In: P. H. Ribbe (ed.). Feldspar Mineralogy (Second Edition). *Reviews in Mineralogy*, vol. 2, 57-99. Mineralogical Society of America, Washington, D.C.

Kroll H., Ribbe P.H. (1987) Determining (Al, Si) distribution and strain in alkali feldspars using lattice parameters and diffraction-peak positions: A review. *American Mineralogist*, vol. 72, 491-506.

Laugier J., Bochu B. Chekcell: Graphical Powder Indexing Cell and Spacegroup Assignment Software, http://www.inpg.gr/LMGP.

Lee M.R., Brown D.J., Smith C.L., Hodson M.E., MacKenzie M., Hellmann R. (2007) Characterization of mineral surfaces using FIB and TEM: A case study of naturally weathered alkali feldspars. *American Mineralogist*, vol. 92, 1383-1394.

Ribbe, P.H. (ed.), (1983) *Feldspar Mineralogy*, 2nd edn. Reviews in Mineralogy, vol. 2, Mineralogical Society of America

Smith, J.V., Brown, W.L. (1988) *Feldspar minerals*, vol. 1. Crystal structures, physical, chemical and microtextural properties. Berlin, Springen Verlag, 828pp.

Theodosoglou E., Koroneos A., Soldatos T., Zorba T., Paraskevopoulos K.M. (2010) Comparative Fourier transform infrared and X-ray powder diffraction analysis of naturally occurred K-feldspars. *Bulletin of the Geological Society of Greece*, Proceedings of the 12th International Congress, Patras, 2752-2761.

Wintle, A.G. (1973) Anomalous fading of thermoluminescence in mineral samples. *Nature*, vol. 245 (21), 143–144.

Zhang M., Salje E.K.H., Carpenter M.A., Parsons I., Kroll H., Reed S.J.B., Graeme-Barber A. (1997) Exsolution and Al-Si disorder in alkali feldspars: Their analysis by infrared spectroscopy. *American Mineralogist*, vol. 82, 849-857.